JCTC Journal of Chemical Theory and Computation

Article

pubs.acs.org/JCTC

How Do Heavier Halide Ligands Affect the Signs and Magnitudes of the Zero-Field Splittings in Halogenonickel(II) Scorpionate Complexes? A Theoretical Investigation Coupled to Ligand-Field Analysis

Shengfa Ye* and Frank Neese*

Max-Planck Institute for Bioinorganic Chemistry, Stiftstrasse 34-36, D-45470 Mülheim an der Ruhr, Germany

Supporting Information

ABSTRACT: This work presents a detailed analysis of the physical origin of the zero-field splittings (ZFSs) in a series of high-spin (S = 1) nickel(II) scorpionate complexes Tp*NiX (Tp* = hydrotris(3,5-dimethylpyrazole)borate, X = Cl, Br, I) using quantum chemical approaches. High-frequency and -field electron paramagnetic resonance studies have shown that the complexes with heavier halide ligands (Br, I) have greater magnitudes but opposite signs of the ZFSs compared with the chloro congener (Desrochers, P. J.; Telser, J.; Zvyagin, S. A.; Ozarowski, A.; Krzystek, J.; Vicic, D. A. *Inorg. Chem.* **2006**, *45*, 8930−8941). To rationalize the experimental findings, quantum chemical calculations of the ZFSs in this Ni^{II} halide series have been conducted. The computed ZFS using wave-function-based ab initio methods (state-averaged CASSCF, NEVPT2, and SORCI) are in good agreement with the experiment. For comparison, density functional theory was only marginally successful. The ligand-field analysis demonstrates that the signs and magnitudes of the ZFSs are subtly determined by the trade-off between the negative contributions from the $^{1,3}A_1(1e\rightarrow 2e)$ transitions relative to the positive contributions from the remaining d-d excited states. The term from $^{1,3}A_1(1e\rightarrow 2e)$ stems from the structural feature that the metal center displaces out of the equatorial plane, and gains the importance when heavier halide ligand is involved.

INTRODUCTION

Ever since the discovery of the slow magnetic relaxation in $Mn_{12}O_{12}(CH_3CO_2)_{16}(H_2O)_4$ below the blocking temperature (T_B), such molecules, known as single molecular magnets (SMMs), have attracted much attention.[1] It is a desirable goal to synthesize a SMM with much higher T_B owing to its potential application as a building block for molecular sized communication devices. The prerequisite condition for a given molecule to exhibit SMM behavior is that the complex has a negative axial zero-field splitting (ZFS) parameter D. It has long been believed that the magnetic relaxation barrier (U), which is proportional to T_B, is governed by the total spin S of the molecular ground state and the absolute magnitude of D, $U = S^2|D|$. However, U is approximately independent of the total spin S, because the D value scales with S as S^{-2}.[2] Although exhaustive attempts aiming at generating a transition metal cluster with higher S by increasing nuclearity have been made, to date, the reported T_B values do not exceed a few Kelvin.[1] Thus, there is considerable debate about the most promising strategy for synthesizing SMMs. Alternatively, mono- or dinuclear transition metal complexes can function as SMMs.[3,4] For example, magnetization measurements revealed the presence of very large D values in a series of high-spin Fe^{II} complexes and hence slow magnetic relaxation in these single-ion systems.[5] Thus, a promising strategy appears to be to employ mono-metallic species with large D values as building blocks for SMMs. However, to achieve a rational design of SMMs, one has to identify key factors that dictate the signs and the magnitudes of D values in mono-metallic systems.

In fact, it is a challenge to understand the physical origin of the ZFSs in transition metal complexes.[6] If one starts from spin-free wave functions and introduces relativistic effects up to second order, the ZFS (**D**-tensor) consists of two contributions: (a) the direct electron−electron spin−spin coupling (SSC) to first order in perturbation theory and (b) the spin−orbit coupling (SOC) to second order in perturbation theory.[7]

The SSC part has long been claimed to give rise to the leading contribution to ZFSs of organic radicals,[8] whereas ZFSs of transition metal complexes are usually dominated by the second-order SOC term.[9] However, the analysis of the **D**-tensors of a range of Mn^{III},[10] V^{III},[11] and Ni^{II}[12] complexes revealed that the SSC term may have contributions of 1−2 cm^{-1}. Hence, for moderate D values, it may be comparable to the SOC part. Thus, the SSC contribution has to be included to reach quantitative results.

In the literature, ligand-field theory (LFT) has been extensively employed to interpret the SOC parts of ZFSs in transition metal compounds.[13] In classical LFT arguments, the ZFS and the g-tensor are usually assumed to be related to a common tensor $\mathbf{\Lambda}$; thus, the g-shift is proportional to the **D**-tensor.[13] However, this long-held assumption is misleading because only excited states with the same total spin ($\Delta S = 0$) as the ground state contribute to the g-shift, whereas the **D**-tensor contains the terms not only from excited states with $\Delta S = 0$ but also from those with $\Delta S = \pm 1$.[14] In addition, LFT treatments

Received: March 22, 2012
Published: May 29, 2012

can only provide a qualitative description of the interactions involved.

Recently, the calculation of ZFSs by first principle electronic structure theory has made significant progress.[15] In the framework of density functional theory (DFT), the first calculation of the SSC term was reported by Petrenko et al.,[16] who adapted the equation of Mcweeny and Mizuno[17] to the case of a single Kohn−Sham determinant. Two implementations are available.[18] Perturbative treatments of the SOC contribution to the ZFS have been worked out by Pederson and Khanna,[19] ourselves,[20] Reviakine et al.,[21] Tekeda et al.,[22] Aquino and Rodriguez,[23] and, most recently, by van Wüllen.[24] However, the calibration studies have shown that DFT methods have met mixed success.[21,25] In some cases, DFT calculations even predict the wrong sign of D.[11] By contrast, wave-function-based ab initio approaches often deliver much better results than DFT methods, especially for transition metal complexes with dominant SOC contributions.[26] In these works, multireference configuration interaction (MRCI), as well as complete active space self-consistent field (CASSCF), together with second-order perturbation theory (CASPT2), have been used. In multi-configurational ab initio calculations, each M_S member of a given multiplet with total spin S can be explicitly represented. The SOC term can be obtained either by simultaneous diagonalization of the Born−Oppenheimer and SOC Hamiltonians[27] or by diagonalization of the SOC Hamiltonian in the space of only a few CI roots.[28] The estimation of the SSC part with highly correlated MRCI wave functions has been developed recently, as well.[29] In "infinite order" treatments of the SOC, the problem arises that a second order bilinear **D**-tensor is not readily obtained. A straightforward procedure to solve this problem is a mapping procedure,[14] but a more rigorous and satisfactory solution is the effective Hamiltonian approach as worked out by Maurice and Guihéry.[30]

High-field electron paramagnetic resonance (EPR) studies on bishalogeno Mn^{II} complexes $Mn(tpa)X_2$ and $Mn(terpy)X_2$ (tpa = tris-2-picolyamine; terpy = 2,2′:6′,2″-terpyridine; X = Cl, Br, I)[31] have shown that the complexes with heavier halides (Br, I) have negative ZFSs, whereas the chloro derivative has a positive one. Variable-field magnetization measurements on $[Cr(dmpe)_2(CN)X]^{+/0}$ (dmpe = 1,2-bis(dimethylphosphino)-ethane) demonstrated substantial increase in D values upon going from Cl to Br to I; however, the signs of D values have not been unambiguously determined.[32] A series of high-spin Ni^{II} scorpionate complexes Tp*NiX (Tp* = hydrotris(3,5-dimethylpyrazole)borate) have been characterized by high-frequency and -field EPR. The results revealed that the bromo and iodo complexes exhibit not only greater magnitudes of D but also the opposite signs relative to the chloro congener.[33] In the present contribution, we have performed quantum chemical calculations using DFT and correlated ab initio methods together with a detailed ligand-field analysis of the ZFSs in the aforementioned nickel complexes in order to rationalize the experimentally observed changes in the signs and the magnitudes of the D values with different halide ligands.

COMPUTATIONAL DETAILS

A truncated ligand model (Tp), in which the two methyl groups on the pyrazole ring of Tp* were replaced by hydrogens, was employed in the calculations. Geometry optimizations were carried out with the BP86[34] density functional. Scalar relativistic effects were taken into account by using the zeroth-order regular approximation (ZORA),[35] our implementation follows the model potential approximation of van Wüllen.[36] The respective ZORA-TZVP basis sets[37] were employed for Ni, Cl, Br, and I, and the ZORA-SV(P) basis sets[37] for the remaining atoms. It has been shown that calculated ZFS parameters may be very sensitive to minor structural changes;[25a] therefore, for NiTpCl and NiTpBr, the calculations of the **D**-tensors were performed at the experimentally determined geometries, as well. In the case of NiTpI, there is no crystal structure available; hence, only the theoretical geometry could be used. To check the effect of the model truncation, the calculations on the untruncated chloro complex was undertaken. It turns out that the results are nearly identical to those for the truncated model with the deviation of D less than 0.2 cm^{-1}.

In a sum-overstates formulation, the SOC contribution to the **D**-tensor consists of three terms that arise from the excited states of the same total spin as the ground state, as well as the excited states, differing by one unit of total spin; explicitly,[14]

$$D_{kl} = D_{kl}^{SSC} + D_{kl}^{SOC(0)} + D_{kl}^{SOC(-1)} + D_{kl}^{SOC(+1)} \tag{1}$$

with

$$D_{kl}^{SOC(0)} = -\frac{1}{S^2}\sum_{b(S_b=S)} \Delta_b^{-1}\langle 0SS|\sum_i h_i^{k,SOC}s_{i,0}|bSS\rangle\langle bSS|\sum_i h_i^{l,SOC}s_{i,0}|0SS\rangle$$

$$D_{kl}^{SOC(-1)} = -\frac{1}{S(2S-1)}\sum_{b(S_b=S-1)} \Delta_b^{-1}\langle 0SS|\sum_i h_i^{k,SOC}s_{i,+1}|bS-1S-1\rangle\langle bS-1S-1|\sum_i h_i^{l,SOC}s_{i,-1}|0SS\rangle$$

$$D_{kl}^{SOC(+1)} = -\frac{1}{(S+1)(2S+1)}\sum_{b(S_b=S+1)} \Delta_b^{-1}\langle 0SS|\sum_i h_i^{k,SOC}s_{i,-1}|bS+1S+1\rangle\langle bS+1S+1|\sum_i h_i^{l,SOC}s_{i,+1}|0SS\rangle \tag{2}$$

Here, S is the total spin of the ground state and the sums over all electronically excited states $|bSS\rangle$ indexed by b of the appropriate total spin.

The calculation of the infinite sum in sum-overstates can be avoided by reformulating the theory in terms of analytic derivatives of the ground state wave function.[38] For the ZFS-tensor, this formalism has been developed recently.[20] The relevant equations read as follows:

$$D_{kl}^{SOC(0)} = -\frac{1}{4S^2}\sum_{\mu\nu}(\mu|h^{k,SOC}|\nu)\frac{\partial P_{\mu\nu}^{(0)}}{\partial x_l^{(0)}}$$

$$D_{kl}^{SOC(-1)} = \frac{1}{2S(2S-1)}\sum_{\mu\nu}(\mu|h^{k,SOC}|\nu)\frac{\partial P_{\mu\nu}^{(+1)}}{\partial x_l^{(-1)}}$$

$$D_{kl}^{SOC(+1)} = \frac{1}{2(S+1)(2S+1)}\sum_{\mu\nu}(\mu|h^{k,SOC}|\nu)\frac{\partial P_{\mu\nu}^{(-1)}}{\partial x_l^{(+1)}} \tag{3}$$

dx.doi.org/10.1021/ct300237f | J. Chem. Theory Comput. 2012, 8, 2344−2351

As elaborated elsewhere,[18b] $P_{\mu\nu}^{(m)}$ $(m = 0, \pm 1)$ correspond to elements of generalized spin densities and $(\mu|h^{k,SOC}|\nu)$ $(k = x, y, z)$ matrix elements of the spatial part of the SOC operator over basis functions ϕ_μ, ϕ_ν. Van Wüllen has recently criticized eq 3.[24] Following the same lines of thought, he arrived at a slightly different expression that has the prefactor $1/(2S(2S-1))$ in front of all three SOC contributions. In our experience, his equation yields results quite close to the original formulation. For comparison, we have applied both procedures here. In the evaluation of SOC integrals, the Breit−Pauli two-electron SOC operator was represented by the spin−orbit mean-field (SOMF) approximation[39] in the implementation of ref 40.

The SSC contributions are calculated from the equation of McWeeny and Mizuno:[17]

$$D_{kl}^{SSC} = \frac{g_e^2}{4}\frac{\alpha^2}{S(2S-1)}\sum_{\mu\nu}\sum_{\kappa\tau}\{P_{\mu\nu}^{\alpha-\beta}P_{\kappa\tau}^{\alpha-\beta} - P_{\mu\kappa}^{\alpha-\beta}P_{\nu\tau}^{\alpha-\beta}\} < \mu\nu|r_{12}^{-5}\{3r_{12,k}r_{12,l} - \delta_{kl}r_{12}\}\kappa\tau> \quad (4)$$

in which the spin density matrix $\mathbf{P}^{\alpha-\beta}$ was obtained on the basis of the spin-unrestricted natural orbital (UNO) determinant.[18b]

The density functional theory (DFT) calculations of the ZFSs of NiTpX were conducted at the ZORA/BP86[34,35] level of theory using the ZORA-TZV(2d,2p) basis set[37] for all atoms.

Quasi-degenerate perturbation theory (QDPT)[28f] was used to calculate ZFSs to verify the DFT results, which is based on ab initio methods such as CASSCF. Again in all ab initio calculations, the ZORA approximation[35] was employed, along with the ZORA-TZV(2d,2p) basis set[37] for all elements. Specifically, in the active space, eight electrons were distributed into the five Ni 3d-based molecular orbitals (CAS(8,5)), and in the CASSCF calculations, the orbitals were optimized by the average of 10 triplet and 15 singlet roots. Diagonalization of the SOC matrix, which is constructed by the state-averaged CASSCF (SA-CASSCF) roots describing the triplet and singlet multiplets of the d^8 configuration, yields the energies of spin−orbit split components of the electronic ground and d-d excited states. Thus, this treatment amounts to an infinite order treatment of the SOC in terms of perturbation theory, and it may be regarded as an ab initio realization of ligand-field theory that takes differential orbital covalency into account as well. The SSC contributions were estimated using the Breit−Pauli spin−spin Hamiltonian in conjunction with first-order perturbation theory.[29b] The RI approximation[29b] was used to speed up the calculations of SSC terms along with the TZV/C auxiliary basis sets.[41] The ZFS parameters were obtained by mapping the energy difference among the ground-state magnetic sublevels into the form of the solution of the $S = 1$ spin-Hamiltonian (eq 5).

$$E(|0\rangle) = 0$$
$$E(|+\rangle) = D + E$$
$$E(|-\rangle) = D - E \quad (5)$$

In addition, the calculations based on the recently developed second-order N-electron valence perturbation theory (NEVPT2)[42] were also performed. In NEVPT2 calculations, the wave functions are the same as those obtained by the SA-CASSCF approach; however, the state energies that enter the QDPT treatment are corrected to second order, obtained from the NEVPT2 calculations.

Moreover, we have carried out more rigorous MRCI calculations in the form of the spectroscopy oriented configuration interaction (SORCI)[43] on the top of CASSCF reference space. In the SORCI calculations, the thresholds T_{pre}, T_{nat}, and T_{sel} were set to 10^{-5}, 10^{-5}, 10^{-6} Eh, respectively.

All calculations in this work were performed with the ORCA program package.[44]

RESULTS

Geometric Structure. As shown in Scheme 1, the TpNiX complexes of the present work contain a four-coordinated Ni^{II} ion in a peudo-tetrahedral coordination environment and hence feature $S = 1$ high-spin ground states. The complexes have C_{3v} symmetry with the 3-fold axis defined by B−Ni−X, which by convention is chosen to be Z-axis in the following discussion. The optimized structures (Table 1) are in good agreement with the experimentally determined geometries. Specifically, the maximum deviations between theory and experiment are only 0.03 Å for the metal−ligand bond lengths and 1 degree for the X−Ni−N_{Tp} angle.

Scheme 1. Structure of TpNiX

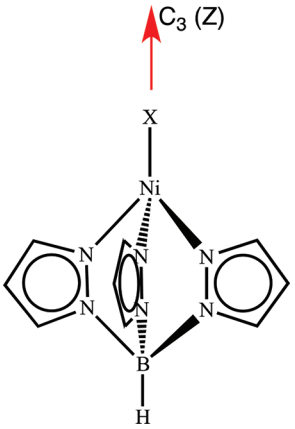

Table 1. Comparison of the Computed Metrical Parameters of NiTpX with the Experimental Crystal Structures (In the Parentheses)

	NiTpCl	NiTpBr	NiTpI
Ni−X (Å)	2.158 (2.170)	2.288 (2.291)	2.471
Ni−N_{Tp} (Å)	1.986 (1.963)	1.984 (1.970)	1.983
X−Ni−N_{Tp} (deg)	124.4 (123.7)	124.3 (123.5)	124.0

DFT Calculations. The calculated ZFS parameters of NiTpX using ZORA/BP86 linear response theory and the individual contributions are tabulated in Table 2. The results demonstrate that for all investigated complexes the SOC terms provide the leading contributions to the final D values and the SSC parts are negligible for these systems. This conclusion is corroborated by the ab initio calculations (see below). Thus, the following discussion will be focused on the SOC contributions only. However, the ZFSs delivered by DFT calculations cannot qualitatively reproduce the signs of the experimental data for the bromo and iodo complexes. The calculations using the equation proposed by van Wüllen[24] yield slightly better results; however, the positive signs of the D values for NiTpBr and NiTpI were also observed (Supporting Information, Table S1). As will be elaborated later, the sign of

Table 2. Calculated ZFS Parameters by the DFT Method for NiTpX[a]

	NiTpCl	NiTpBr	NiTpI
D_{exp} (cm^{-1})	3.9	−11.4	−22.8
D_{cal} (cm^{-1})	2.6 (2.7)	25.5 (26.7)	125.9
D^{SOC} (cm^{-1})	2.5 (2.6)	25.3 (26.6)	125.9
$\alpha\rightarrow\alpha$	1.2 (1.0)	8.4 (8.5)	19.2
$\beta\rightarrow\beta$	−1.1 (−1.3)	−12.6 (−12.4)	−55.0
$\alpha\rightarrow\beta$	2.9 (3.3)	33.2 (33.9)	174.1
$\beta\rightarrow\alpha$	−0.5 (−0.4)	−3.7 (−3.4)	−12.4
D^{SSC} (cm^{-1})	0.1 (0.1)	0.1 (0.1)	0

[a]The corresponding values for the crystal structures are in the parentheses.

the D value is subtly determined by the trade-off between the negative contribution from the doubly occupied molecular orbital (DOMO) to singly occupied molecular orbital (SOMO) transitions ($\beta\rightarrow\beta$) and the positive one from spin-flip transitions ($\alpha\rightarrow\beta$). In line with this, the DFT calculations also predict that the values of the other two contributions ($D^{\alpha\alpha}$ and $D^{\beta\alpha}$) are quite small and nearly canceling (Table 2). Therefore, in the case of the bromo and iodo complexes, the DFT calculations may substantially overestimate the positive contribution from the spin-flip transitions, which may be readily ascribed to the well-known limitation of single determinant methods such as DFT in describing spin-flip phenomena.[45] Since there is a large systematic error in DFT calculations, more rigorous ab initio methods had to be used to compute the ZFSs in NiTpX.

Ab Initio Calculations. To circumvent the shortcomings inherent to DFT methods, multi-determinantal methods are the alternatives of choice. The most feasible starting point is the CASSCF method. Based on previous experience with only moderately covalent transition metal complexes, the smallest reasonable active space consists of eight active electrons in the five metal d-based orbitals (CAS(8,5)). In the CASSCF and NEVPT2 calculations, all d-d excited states arising from the d^8 configuration (10 triplet and 15 singlet states) were explicitly computed and then included into the QDPT procedure. In addition, computationally much more demanding SORCI calculations on top of the CASSCF reference space were carried out.

In sharp contrast to the DFT results, the computed ZFS-tensors obtained by using ab initio methods (Table 3) agree much better with experiment for all nickel complexes under investigation. Specifically, the ab initio calculations reproduce not only the sign but also the magnitude of the **D**-tensors. As might have been anticipated based on past experience, the CASSCF and NEVPT2 methods perform as well as the much more elaborate SORCI approach, since the metal−ligand interaction is considerably ionic. In addition, no superiority of the experimentally determined geometries for the calculations of the ZFSs was observed. This may be due to the fact that the computed geometries are in excellent agreement with the available crystal structures (Table 1).

Electronic Structure. To understand the physical origin of the ZFSs in the investigated nickel complexes, one has to analyze the electronic structures of the ground and d-d excited states in some detail. Among the relevant excited states, single excitations deserve particular attention because they are the most important contributors to the ZFS owing to the fact that the SOC operator is represented by an effective one-particle interaction. Hence, only states that are dominated by single excitations from the ground state will strongly couple to the latter via SOC.

As expected from LFT, trigonally distorted tetrahedral coordination geometries (C_{3v} point group) of NiTpX lead to a $^3A_2$ ground state due to single occupation of the degenerate $d_{xz,yz}$-based π^*-orbitals. However, as depicted in Figure 1 for NiTpCl, the SOMOs contain a significant contribution from the other e-set (d_{xy,x^2-y^2}). Analogous results were obtained for NiTpBr and NiTpI. As analyzed for the related Ni and V complexes with the similar coordination environments,[11,12] this considerable mixing of the two e-sets is due to the geometric feature of the complexes: the substantial displacement of the metal center out of the equatorial plane defined by the three N_{Tp} atoms (∼ 1.1 Å). The important d-d excited states are the following: promotion of one electron from the Ni d_{z^2}-based orbital ($1a_1$) to the 2e-set gives rise to a singlet ($^1E(1a_1\rightarrow 1e)$) and a triplet ($^3E(1a_1\rightarrow 1e)$) excited state. The single excitation from the 1e-MOs to the 2e-set results in three triplet excited states $^3A_1(1e\rightarrow 2e)$, $^3A_2(1e\rightarrow 2e)$, and $^3E(1e\rightarrow 2e)$, as well as three singlet excited states of the same symmetry. In addition, there are two singlet excited states of $^1A_1(2e\rightarrow 2e)$ and $^1E(2e\rightarrow 2e)$ symmetry arising from the spin-flip transitions within the degenerate SOMOs.

Ligand-Field Analysis. To assist in the interpretation of the results obtained from the ab initio calculations, we carried out a detailed ligand-field analysis about the origin of the ZFS. To treat the SOC of the halide ligand on the same footing as the SOC of the metal center, the metal 3d-based MOs can be written as

$$
\begin{aligned}
1e_x &\cong \alpha^{M}_{xy,x^2-y^2} d_{xy} + \alpha^{M}_{xz,yz} d_{xz} + \alpha^{L}_{x,y} p_x \\
1e_y &\cong \alpha^{M}_{xy,x^2-y^2} d_{x^2-y^2} + \alpha^{M}_{xz,yz} d_{yz} + \alpha^{L}_{x,y} p_y \\
1a_1 &\cong \beta^{M}_{z^2} d_{z^2} + \beta^{L}_{z} p_z \\
2e_x &\cong \gamma^{M}_{xz,yz} d_{xz} + \gamma^{M}_{xy,x^2-y^2} d_{xy} + \gamma^{L}_{x,y} p_x \\
2e_y &\cong \gamma^{M}_{xz,yz} d_{yz} + \gamma^{M}_{xy,x^2-y^2} d_{x^2-y^2} + \gamma^{L}_{x,y} p_y
\end{aligned}
\tag{5}
$$

Table 3. Calculated ZFS Parameters Using Ab Initio Methods for NiTpX[a]

	NiTpCl			NiTpBr			NiTpI		
D_{exp} (cm^{-1})	3.9			−11.4			−22.8		
method	CASSCF	NEVPT2	SORCI	CASSCF	NEVPT2	SORCI	CASSCF	NEVPT2	SORCI
D_{cal} (cm^{-1})	3.9 (3.8)	3.8 (3.9)	2.0 (4.9)	−6.8 (−6.6)	−6.9 (−6.9)	−9.6 (−9.7)	−19.1	−19.6	−21.5
D^{SOC} (cm^{-1})	3.9 (3.7)	3.8 (3.8)	1.8 (4.8)	−6.8 (−6.6)	−6.9 (−6.9)	−9.6 (−9.7)	−18.9	−19.4	−21.2
D^{SSC} (cm^{-1})	0 (0.1)	0 (0.1)	0.2 (0.1)	0 (0)	0 (0)	0 (0)	−0.2	−0.2	−0.2

[a]The corresponding values for the crystal structures are in the parentheses.

dx.doi.org/10.1021/ct300237f | J. Chem. Theory Comput. 2012, 8, 2344−2351

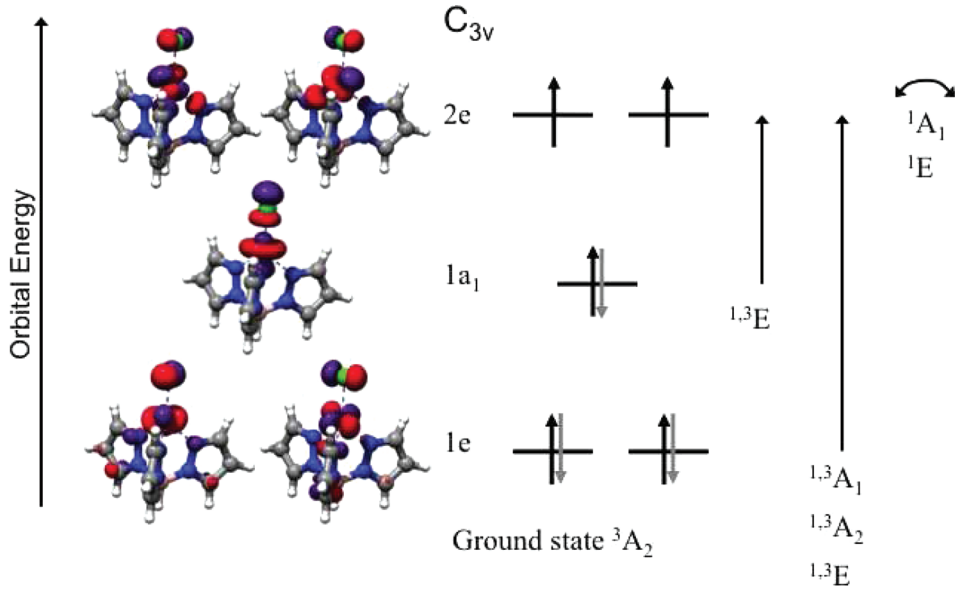

Figure 1. The metal d-based MOs and term symbols arising from single excitations for NiTpCl. The indicated orbital occupation pattern corresponds to the $^3A_2$ ground state.

Here, α_i^M, β_i^M, and γ_i^M, and as well as α_i^L, β_i^L, and γ_i^L, are the fractional nickel 3d-orbital and halide p-orbital character of the indicated type in the metal 3d-based MOs, respectively.

The wave functions used in the treatments are then given by

$$
\begin{aligned}
|^3A_2(g.\,s.)\rangle &= |(\text{core})2e_x2e_y| \\
|^1A_1(2e \rightarrow 2e)\rangle &= \frac{1}{\sqrt{2}}(|(\text{core})2e_x\overline{2e_x}| + |(\text{core})2e_y\overline{2e_y}|) \\
|^1E(2e \rightarrow 2e)\rangle &= \begin{cases} \frac{1}{\sqrt{2}}(|(\text{core})2e_x\overline{2e_x}| - |(\text{core})2e_y\overline{2e_y}|) \\ \frac{1}{\sqrt{2}}(|(\text{core})2e_x\overline{2e_y}| - |(\text{core})\overline{2e_x}2e_y|) \end{cases} \\
|^3E(1e \rightarrow a_1)\rangle &= \begin{cases} |(\text{core})1a_12e_x| \\ |(\text{core})1a_12e_y| \end{cases} \\
|^3A_1(1e \rightarrow 2e)\rangle &= \frac{1}{\sqrt{2}}(|(\text{core})1e_x2e_x| + |(\text{core})1e_y2e_y|) \\
|^3A_2(1e \rightarrow 2e)\rangle &= \frac{1}{\sqrt{2}}(|(\text{core})1e_y2e_x| - |(\text{core})1e_x2e_y|) \\
|^3E(1e \rightarrow 2e)\rangle &= \begin{cases} \frac{1}{\sqrt{2}}(|(\text{core})1e_y2e_x| + |(\text{core})1e_x2e_y|) \\ \frac{1}{\sqrt{2}}(|(\text{core})1e_x2e_x| - |(\text{core})1e_y2e_y|) \end{cases}
\end{aligned}
\tag{6}
$$

Here, an orbital with an overbar is occupied with a spin-down electron, |...| denotes a normalized Slater determinant, and (core) represents the inactive doubly occupied MOs of the system. For clarity, the doubly occupied metal d-based MOs are omitted in the Slater determinant.

Using the ligand-field type argument, as explained in ref 46, one readily derives an equation for the ZFSs of the investigated nickel complexes.

$$
\begin{aligned}
D^{SOC}(^3A_2) \cong\ & \frac{\{\zeta_{Ni}[(\gamma^M_{xz,yz})^2 - 2(\gamma^M_{xy,x^2-y^2})^2] + \zeta_X(\gamma^L_{x,y})^2\}^2}{\Delta(^1A(2e \rightarrow 2e))} \\
& + \frac{1}{4}\frac{[\zeta_{Ni}(\sqrt{3}\beta^M_{z^2}\gamma^M_{xz,yz}) + \zeta_X\beta^L_z\gamma^L_{x,y}]^2}{\Delta(^3E(1a_1 \rightarrow 2e))} \\
& - \frac{1}{4}\frac{[\zeta_{Ni}(\sqrt{3}\beta^M_{z^2}\gamma^M_{xz,yz}) + \zeta_X\beta^L_z\gamma^L_{x,y}]^2}{\Delta(^1E(1a_1 \rightarrow 2e))} \\
& - \frac{1}{2}\frac{[\zeta_{Ni}(2\alpha^M_{xy,x^2-y^2}\gamma^M_{xy,x^2-y^2} - \alpha^M_{xz,yz}\gamma^M_{xz,yz}) - \zeta_X\alpha^L_{x,y}\gamma^L_{x,y}]^2}{\Delta(^3A_1(1e \rightarrow 2e))} \\
& + \frac{1}{2}\frac{[\zeta_{Ni}(2\alpha^M_{xy,x^2-y^2}\gamma^M_{xy,x^2-y^2} - \alpha^M_{xz,yz}\gamma^M_{xz,yz}) - \zeta_X\alpha^L_{x,y}\gamma^L_{x,y}]^2}{\Delta(^1A_1(1e \rightarrow 2e))} \\
& + \frac{1}{2}\frac{[\zeta_{Ni}(\alpha^M_{xz,yz}\gamma^M_{xy,x^2-y^2} - \alpha^M_{xy,x^2-y^2}\gamma^M_{xz,yz})]^2}{\Delta(^3E(1e \rightarrow 2e))} \\
& - \frac{1}{2}\frac{[\zeta_{Ni}(\alpha^M_{xz,yz}\gamma^M_{xy,x^2-y^2} - \alpha^M_{xy,x^2-y^2}\gamma^M_{xz,yz})]^2}{\Delta(^1E(1e \rightarrow 2e))}
\end{aligned}
\tag{7}
$$

Here, ζ_{Ni} and ζ_X are the one-electron SOC constants for a Ni 3d-electron and for a halide valence p-electron, respectively. $\Delta(X)$ is the transition energy from the ground state to excited state X. As shown in eq 7, there are contributions from several pairs of the excited states $^{1,3}X$. If a given excited state ^3X gives a positive contribution to the D value, the corresponding singlet counterpart ^1X with the same spatial part but different spin coupling yields a compensating negative one, and vice visa. Obviously, the intra-SOMO transition $^1A_1(2e\rightarrow2e)$ has no triplet partner and yields an uncompensated positive contribution. In effect, only the pair of the single excitations $^{1,3}A_1(1e\rightarrow2e)$ leads to a negative contribution, whereas all other excited states together make a positive one. Given the complex nature of eq 7, the magnitudes of the contributions are largely affected by the metal−ligand covalency, and more subtly, by the mixing degree of the two e-sets. Thus, one cannot reach any quantitative conclusion just by simple inspection of eq 7.

Based on the transition energies obtained from the CASSCF, NEVPT2 and SORCI calculations and the SOC matrix

Table 4. Calculated Excitation Energies for Key d-d Excited States for TpNiX (the Available Experimental Data in Parentheses) and Their Corresponding Contributions to the D Value

	NiTpCl		NiTpBr		NiTpI	
state	energy (cm^{-1})	contribution to D (cm^{-1})	energy (cm^{-1})	contribution to D (cm^{-1})	energy (cm^{-1})	contribution to D (cm^{-1})
$^1A_1(2e\rightarrow 2e)$	21900	13.9	23690	8.5	22780	4.1
$^1E(2e\rightarrow 2e)$	14780	0	16660	0	16830	0
$^3E(1a_1\rightarrow 2e)$	6110 (6290)	55.8	6160 (6290)	45.9	6010 (6420)	49.2
$^1E(1a_1\rightarrow 2e)$	20600	−14.6	21800	−9.0	22150	−4.5
$^3A_1(1e\rightarrow 2e)$	6700	−54.4	7160	−55.9	6500	−70.1
$^1A_1(1e\rightarrow 2e)$	22670	0.9	22560	0.7	25620	0.2
$^3E(1e\rightarrow 2e)$	10730 (11200)	0.5	10510 (11110)	0.5	9800 (10890)	0.5
$^1E(1e\rightarrow 2e)$	26120	−0.3	27820	−0.3	28560	−0.5
$^3A_2(1e\rightarrow 2e)$	11400 (12520)	0	11540 (12320)	0	10770 (11980)	0
Total D^{SOC}		1.8		−9.6		−21.2

elements computed in the QDPT procedures, we can directly calculate the contribution from each excited state without involving the complexities of extracting the parameters such as α_i, β_i, and γ_i The results are summarized in Table 4. Since the CASSCF, NEVPT2, and SORCI methods predict essentially identical D values for all complexes in this work, the following analysis was only conducted on the basis of the SORCI results.

The calculated excitation energies match the available experimental date reasonably well (Table 4). The computed contributions from all excited states corroborate the arguments deduced from the ligand-field analysis. The delicate balance among numerous contributions determines the final sign of D. Thus, the D value cannot be determined a priori without conducting electronic structure calculations.

If there are very low-lying d-d excited multiplets, one may anticipate that these excited states certainly make the most important contributions to the ZFS. Indeed, $^3E(1a\rightarrow 2e)$ and $^1A_1(1e\rightarrow 2e)$ are the most important contributors of all spin-conserving transitions. By contrast, due to the symmetry reason, the lowest-energy singlet excited state $^1E(2e\rightarrow 2e)$ cannot couple to the ground state via SOC and hence has a vanishing contribution to D. However, the spin-flip transitions $^1A_1(2e\rightarrow 2e)$ and $^1E(1a\rightarrow 2e)$ with higher excitation energies yield non-negligible contributions, especially for NiTpCl and NiTpBr. Other transitions typically occur at relatively high excitation energies, which quench their contributions. This result is counter to the common assumption that ZFS is often dominated by excited states of the same spin as the ground state, at least in non-Kramers systems.

In comparison with NiTpCl, the change in the sign of the D value for the bromo analogue results from the considerable decrease in the positive contributions from $^1A_1(2e\rightarrow 2e)$ and $^3E(1a\rightarrow 2e)$ relative to the slightly reduced negative contributions from $^3A_1(1e\rightarrow 2e)$ and $^1E(1a\rightarrow 2e)$ (Table 4). Going from Cl and Br to I, there is a big jump for the contribution from the excited state $^3A_1(1e\rightarrow 2e)$, which largely determines the final sign and magnitude of the D value for the iodo derivative.

Owing to the fact that the SOC constants of heavier halide ($\zeta_{Cl^-} \sim 587\ cm^{-1}$, $\zeta_{Br^-} \sim 2457\ cm^{-1}$ and $\zeta_{I^-} \sim 5069\ cm^{-1}$[47]) are much larger than that of Ni^{II} center (688 cm^{-1}[48]), and that the Ni-X covalency is nearly identical for the nickel complexes under investigation, one may expect that the contribution from a given excited state would increase as the heavier halide is involved. However, from Table 4, we have not observed such a trend except the contribution from $^3A_1(1e\rightarrow 2e)$. This is may be due to the rather ionic nature of the Ni-X interaction ($\alpha^L_{x,y} \sim 0.1$, $\beta^L_z \sim 0.03$, $\gamma^L_{x,y} \sim 0.1$), which dramatically reduces the effect of the ligand SOC, and the subtle dependence of the mixing degree of the two e-sets.

DISCUSSION AND CONCLUSION

In this work, a detailed quantum chemical and ligand-field analysis of the physical origin of the ZFSs in a series of four-coordinate Ni^{II} scorpionate complexes has been reported.

Ab initio calculations employ spin eigenfunctions to construct the wave functions and hence are able to properly describe the spin coupling and multiplet effects of transition metal ions. The D values delivered by the CASSCF, NEVPT2, and SORCI calculations are in excellent agreement with experiment. By contrast, DFT computations yield qualitatively wrong results. Specifically, the predicted signs for the bromo and iodo derivatives are opposite to those determined experimentally.

The ligand-field analysis based on the ab initio results enabled us to investigate why the sign and the magnitude of D changes within the halide series. Equation 7 indicates that there are contributions from several pairs of the excited state $^{1,3}X$, and that the final sign of D is determined by the trade-off between the only negative contributions from $^{1,3}A_1(1e\rightarrow 2e)$ relative to those from the remaining d-d excited states. The contribution from $^{1,3}A_1(1e\rightarrow 2e)$ originates from the mixing of the two e-sets. If taking $\alpha^M_{xz,yz}$ and $\alpha^L_{x,y}$ in the 1e-set as well as γ^M_{xy,x^2-y^2} and $\gamma^L_{x,y}$ in the 2e-MOs to be zero in eq 7, one obtains an equation in which the contributions from $^{1,3}A_1(1e\rightarrow 2e)$ completely vanish. Hence, the D values would always be predicted to be positive, irrespective of the nature of the halide ligand.[33] The mixing of the two e-sets is readily ascribed to the large displacement of the Ni center out of the plane defined by the three N-atoms. If the metal center situated at the equatorial plane, the 1e-set are pure $d_{xy,x2-y2}$ orbitals, and accordingly the 2e-set are pure $d_{xz,yz}$ orbitals. The situation is similar to D_{3h} limit where the two e-sets belong to two different irreducible representations; hence, the mixing is symmetrically forbidden. In C_{3v} symmetry, the orbital angular momentum operators $L_{x,y}$ transform as E, and L_z as A_2, respectively. Therefore, out-of-state SOC of the $^{1,3}A_1$ excited states with the $^3A_2$ ground state is only possible via the L_z-component. If there were no mixing of the two e-sets, the metal-related term in the contribution from $^{1,3}A_1(1e\rightarrow 2e)$ would vanish because the $d_{xz,yz}$-based 2e-orbitals cannot couple through L_z with the 1e-set that is mainly of $d_{xy,x2-y2}$ character.

In fact, the contribution from the $^{1,3}A_1(1e\rightarrow 2e)$ excited states to the final D values gains more importance when the heavier

halide is involved (Table 4). If one were to neglect the ligand SOC, the contribution of the $^3A_1(1e\rightarrow 2e)$ excited state would be significantly underestimated, especially for the iodo derivative. Thus, similar to the situation in the chloro analogue, a positive D value would be predicted for bromo and iodo complexes as well. In fact, the previous ligand-field calculations based on the angular overlap model yield the positive D values for bromo and iodo complex, although they succeeded in reproducing the ZFS for chloro derivative.[33] However, the effect of much larger SOC constants of the heavier halide ligand compared to the metal center is substantially reduced by the rather ionic nature of the Ni-X interaction in this series of the nickel complexes. Thus, increasing the covalency of the Ni−Br/I bonds should lead to more negative D values. This may point to a direction for further synthetic effort in order to generate more promising SMMs.

Given the important role of the SOC of the heavier ligand, one may argue that the metal-related part in eq 7 could be left out of the treatment. If this would be done, the cross term arising from expanding the square in eq 7 would be missing. As discussed previously for $FeCl_4^-$,[14] and $Mn(NH_3)_4Br_2$,[31a] such interference contributions have about the same magnitude as D itself. Hence, the metal-related term has to be considered in order to reach quantitative results of D values.

The present work highlights the importance of the SOC contribution of heavier halogens that is capable of overriding the contribution from the metal center. This is not an isolated phenomenon.[49] In addition to the examples mentioned in Introduction, Collingwood et al. reported that the halogen becomes the dominant SOC contributor in $[NiI_4]^{2+}$.[50] Atanasov et al. have shown that for $[NiX_4]^{2+}$ with T_d and distorted D_{2d} symmetry, the halogen SOC contribution has the opposite sign to the metal contribution.[51] Elongated octahedral Mn^{III} complexes almost invariably have negative D values; however, to our knowledge, $[Mn(cyclam)I_2]I$ (cyclam =1,4,8,11-tetraazacyclotetradecane) is an only one exception.[52]

In summary, the final signs and magnitudes of D's in the halogenonickel(II) scorpionate complexes are largely determined by the metal−ligand covalency and low symmetry effects. To accurately predict D values, one has to employ a method that is capable of taking these two factors properly into account. In addition, DFT methods have an intrinsic problem in describing multiplets of transition metal ions. Therefore, ab initio calculations typically yield better results than DFT. The analysis of the contribution from each excited state revealed that numerous d-d excited states contribute to the final D value with similar magnitude but varying signs and different physical origins. The delicate balance among them yields the overall ZFSs. The only negative contribution comes from the pair of $^{1,3}A_1(1e\rightarrow 2e)$ excited state, while the remaining excited states in total make a positive contribution. This negative term ($^{1,3}A_1(1e\rightarrow 2e)$) originates from mixing of the two e-sets induced by the structural feature that the metal center displaces out of the equatorial plane, and gains the importance when heavier halide ligand is involved. However, in the present cases, the limited metal−ligand covalency prohibits the full manifestation of the much stronger SOC effect of heavier ligands. Finally, we hope that the present-day theoretical chemistry will provide reliable correlations between structural features and ZFSs for a wider range of situations with different electronic structures and these correlations are able to guide synthetic efforts toward rational designs in the field of SMMs.

■ ASSOCIATED CONTENT

Supporting Information

The transformation properties of d-orbitals under C_{3v} symmetry, calculated ZFS parameters using van Wüllen's equation for NiTpX, and comparison of d-d excitation energies for NiTpCl predicted by the CASSCF, NEVPT2, and SORCI calculations. This material is available free of charge via the Internet at http://pubs.acs.org.

■ AUTHOR INFORMATION

Corresponding Author

*E-mail: shengfa.ye@mpi-mail.mpg.de, frank.neese@mpi-mail.mpg.de.

Notes

The authors declare no competing financial interest.

■ ACKNOWLEDGMENTS

The authors gratefully acknowledge financial support from the collaborative research center SFB 813 ("Chemistry at spin centers"). We dedicate this paper to Prof. Dr. W. Kaim (University of Stuttgart) on the occasion of his 60th birthday.

■ REFERENCES

(1) (a) Gatteschi, D.; Sessoli, R.; Villain, J. *Molecular Nanomagnets*; Oxford University Press: Oxford, U.K., 2006, pp 108−159. (b) *Single-Molecule Magnets and Related Phenomena. Structure and Bonding*; Winpenny, R., Ed.; Springer: Berlin, 2006; Vol. *122*, pp 1−262.

(2) (a) Waldman, O. *Inorg. Chem.* **2007**, *46*, 10035−10037. (b) Neese, F.; Pantazis, D. A. *Faraday Discuss.* **2011**, *148*, 229−238.

(3) (a) Ishikawa, N.; Sugita, M.; Ishikawa, T.; Koshihara, S.; Kaizu, Y. *J. Am. Chem. Soc.* **2003**, *125*, 8694−8695. (b) AlDamen, M. A.; Clemente-Juan, J. M.; Coronado, E.; Marti-Gastaldo, C.; Gaita-Arino, A. *J. Am. Chem. Soc.* **2008**, *130*, 8874−8875. (c) Rinehart, J. D.; Long, J. R. *J. Am. Chem. Soc.* **2009**, *131*, 12558−12559. (d) Li, D.-P.; Wang, T.-W.; Li, C.-H.; Liu, D.-S.; Li, Y.-Z.; You, X.-Z. *Chem. Commun.* **2010**, *46*, 2929−2931. (e) Jiang, S.-D.; Wang, B.-W.; Sun, H.-L.; Wang, Z.-M.; Gao, S. *J. Am. Chem. Soc.* **2011**, *132*, 4730−4733.

(4) (a) Kajiwara, T.; Nakano, M.; Takaishi, S.; Yamashita, M. *Inorg. Chem.* **2008**, *47*, 8604−8606. (b) Long, J.; Habib, F.; Lin., P.-H.; Korobkov, I.; Enright, G.; Ungur, L.; Wernsdorfer, W.; Chibotaru, L. F.; Murugesu, M. *J. Am. Chem. Soc.* **2011**, *132*, 5319−5328.

(5) (a) Freedman, D. E.; Harman, W. H.; Harris, T. D.; Long, J. R.; Chang, C. J. *J. Am. Chem. Soc.* **2010**, *132*, 1224−1225. (b) Harman, W. H.; Harris, T. D.; Freedman, D. E.; Fong, H.; Chang, A.; Rinehart, J. D.; Ozarowski, A.; Sougrati, M. T.; Grandjean, F.; Long, G. J.; Long, J. R.; Chang, C. J. *J. Am. Chem. Soc.* **2010**, *132*, 18115−18126.

(6) (a) Boča, R. *Coord. Chem. Rev.* **2004**, *248*, 757−815. (b) Titiš, J.; Boča, R. *Inorg. Chem.* **2010**, *49*, 3971−3973.

(7) McWeeny, R. *Methods of Molecular Quantum Mechanics*; Academic Press: London, 1992; pp 357−418.

(8) Schweiger, A.; Jeschke, G. *Principle of Pulse Electron Paramagnetic Resonance*; Oxford University Press: Oxford, U.K., 2001; p 32.

(9) Griffith, J. S. *The Theory of Transition Metal Ions*; Cambridge University Press: Cambridge, 1964; pp 330.

(10) (a) Neese, F. *J. Am. Chem. Soc.* **2006**, *128*, 10213−10222. (b) Duboc, C.; Ganyushin, D.; Sivalingam, K.; Collomb, M.-N.; Neese, F. *J. Phys. Chem. A* **2010**, *114*, 10750−10758.

(11) Ye, S.; Neese, F.; Chu, W.-C.; Smirnov, A.; Ozarowski, D.; Tsai, Y.-F.; Wang, R.-C.; Chen, K.-Y.; Liao, J.-H.; Hung, C.-H.; Telser, J.; Krzystek, J.; Hsu, H.-F. *Inorg. Chem.* **2010**, *49*, 977−988.

(12) Desrochers, P. J.; Sutton, C. A.; Abrams, M. L.; Ye, S.; Neese, F.; Telser, J.; Ozarowski, A.; Krzystek, J. *Inorg. Chem.* **2012**, *51*, 2793−2805.

(13) (a) McGarvey, B. R. *Transition Met. Chem.* **1966**, *3*, 89−201. (b) Abagam, A.; Bleaney, B. *Electron Paramagnetic Resonance of Transition Ions*; Clarendon Press: Oxford, 1970; pp 365−490.

(14) Neese, F.; Solomon, E. I. *Inorg. Chem.* **1998**, *37*, 6568−6582.
(15) Neese, F. In *Calculation of NMR and EPR Parameters. Theory and Applications*; Kaupp, M., Bühl, M., Malkin, V. G., Eds.; Wiley-VCH: Weinheim, Germany, 2004; pp 541−564.
(16) Petrenko, T. T.; Petrenko, T. L.; Bratus, V. Y. *J. Phys.: Condens. Matter* **2002**, *14*, 12433−12440.
(17) McWeeny, R.; Mizuno, Y. *Proc. R. Soc. London* **1961**, *259*, 554−577.
(18) (a) Shoji, M.; Koizumi, K.; Hamamoto, T.; Taniguchi, T.; Takeda, R.; Kitagawa, Y.; Kawakami, T.; Okumura, M.; Yamanaka, S.; Yamaguchi, K. *Polyhedron* **2005**, *24*, 2708−2715. (b) Sinnecker, S.; Neese, F. *J. Phys. Chem. A* **2006**, *110*, 12267−12275.
(19) Pederson, M. R.; Khanna, S. N. *Phys. Rev. B* **1999**, *60*, 9566−9572.
(20) Neese, F. *J. Chem. Phys.* **2007**, *127*, 164112.
(21) Reviakine, R.; Arbuznikov, A. V.; Tremblay, J.-C.; Remenyi, C.; Malkina, O. L.; Malkin, I.; Kaupp, M. *J. Chem. Phys.* **2006**, *125*, 054110.
(22) Takeda, R.; Mitsuo, S.; Yamanaka, S.; Yamaguchi, K. *Polyhedron* **2005**, *24*, 2238−2241.
(23) Aquino, F.; Rodriguez, J. H. *J. Chem. Phys.* **2005**, *123*, 204902.
(24) Schmitt, S.; Jost, P.; van Wüllen, C. *J. Chem. Phys.* **2011**, *134*, 194113.
(25) (a) Zein, S.; Duboc, C.; Lubitz, W.; Neese, F. *Inorg. Chem.* **2008**, *47*, 134−142. (b) Zein, S.; Neese, F. *J. Phys. Chem. B* **2008**, *112*, 7976−7983. (c) Kortus, J. *Phys. Rev. B* **2002**, *66*, 092403.
(26) (a) Liakos, D. G.; Ganyushin, D.; Neese, F. *Inog. Chem.* **2009**, *48*, 10572−10580. (b) Sundararajan, M.; Ganyushin, D.; Ye, S.; Neese, F. *Dalton Trans.* **2009**, 6021−6036. (c) Maurice, R.; de Graaf, C.; Guihéry, N. *J. Chem. Phys.* **2010**, *133*, 084307. (d) Maurice, R.; Pradipto, A. M.; Guihéry, N.; Broer, R.; de Graaf, C. *J. Chem. Theory Comput.* **2010**, *6*, 3092−3101. (e) Maurice, R.; Sivalingam, K.; Ganyushin, D.; Guihéry, N.; de Graaf, C.; Neese, F. *Inorg. Chem.* **2011**, *50*, 6229−6236. (f) Chibotaru, L.; Ungur, L.; Aronica, C.; Elmoll, H.; Pilet, G.; Luneau, D. *J. Am. Chem. Soc.* **2008**, *130*, 12445−12455. (g) Chibotaru, L.; Ungur, L.; Soncini, A. *Angew. Chem., Int. Ed.* **2008**, *47*, 4126−4129. (h) Ungur, L.; Chibotaru, L. F. *Phys. Chem. Chem. Phys.* **2011**, *13*, 20086−20090.
(27) (a) Kleinschmidt, M.; Tatchen, J.; Marian, C. M. *J. Chem. Phys.* **2006**, *124*, 124101. (b) Kleinschmidt, M.; Marian, C. M. *Chem. Phys.* **2005**, *311*, 71−79.
(28) (a) Malmqvist, P.-Å; Roos, B. O.; Schimmelpfennig, B. *Chem. Phys. Lett.* **2002**, *357*, 230−240. (b) Roos, B. O.; Malmqvist, P.-Å. *Phys. Chem. Chem. Phys.* **2004**, *6*, 2919−2927. (c) Berning, A.; Schweizer, M.; Werner, H. J.; Knowles, P. J.; Palmieri, P. *Mol. Phys.* **2000**, *98*, 1823−1833. (d) Tilson, J. L.; Ermler, W. C.; Pitzer, R. M. *Comput. Phys. Commun.* **2000**, *128*, 128−138. (e) Fedorov, D. G.; Koseki, S.; Schmidt, M. W.; Gordon, M. S. *Int. Rev. Phys. Chem.* **2003**, *22*, 551−592. (f) Ganyushin, D.; Neese, F. *J. Chem. Phys.* **2006**, *125*, 024103. (g) Sugisaki, K.; Toyota, K.; Sato, K.; Shiomi, D.; Kitagawa, M.; Takui, T. *Chem. Phys. Lett.* **2009**, *477*, 369−373. (h) Havlas, Z.; Michl, J. *J. Chem. Soc., Perkin Trans. 2* **1999**, 2299−2303. (i) Vahtras, O.; Loboda, O.; Minaev, B.; Ågren, H.; Ruud, K. *Chem. Phys.* **2002**, *279*, 133−142. (j) Loboda, O.; Minaev, B.; Vahtras, O.; Schimmelpfennig, B.; Ågren, H.; Ruud, K.; Jonsson, D. *Chem. Phys.* **2003**, *286*, 127−137. (k) de Graaf, C.; Sousa, C. *Int. J. Quantum Chem.* **2006**, *106*, 2470−2478.
(29) (a) Gilka, N.; Taylor, P. R.; Marian, C. M. *J. Chem. Phys.* **2008**, *129*, 044102. (b) Ganyushin, D.; Gilka, N.; Taylor, P. R.; Neese, F. *J. Chem. Phys.* **2010**, *132*, 144111.
(30) Maurice, R.; Bastardis, R.; Graaf, C.; de; Suaud, N.; Mallah, T.; Guihéry, N. *J. Chem. Theory Comput.* **2009**, *5*, 2977−2984.
(31) (a) Duboc, C.; Phoeung, T.; Zein, S.; Pécaut, J.; Collomb, M.-N.; Neese, F. *Inorg. Chem.* **2007**, *46*, 4905−4916. (b) Mantel, C.; Baffert, C.; Romero, I.; Deronzier, A.; Pécaut, J.; Collomb, M.-N.; Duboc, C. *Inorg. Chem.* **2004**, *43*, 6455−6463.
(32) Karunadasa, H. I.; Arquero, K. D.; Berben, L. A.; Long, J. R. *Inorg. Chem.* **2010**, *49*, 4738−4740.
(33) Desrochers, P. J.; Telser, J.; Zvyagin, S. A.; Ozarowski, A.; Krzystek, J.; Vicic, D. A. *Inorg. Chem.* **2006**, *45*, 8930−8941.
(34) (a) Becke, A. D. *Phys. Rev. A* **1988**, *38*, 3098−3100. (b) Perdew, J. P. *Phys. Rev. B* **1986**, *34*, 7406. (c) Perdew, J. P. *Phys. Rev. B* **1986**, *33*, 8822−8824.
(35) (a) van Lenthe, E.; Baerends, E. J.; Snijders, J. G. *J. Chem. Phys.* **1993**, *99*, 4597−4610. (b) van Lenthe, E.; Baerends, E. J.; Snijders, J. G. *J. Chem. Phys.* **1994**, *101*, 9783−9792. (c) van Lenthe, E.; van Leeuwen, R.; Baerends, E. J.; Snijders, J. G. *Int. J. Quantum Chem.* **1996**, *57*, 281−293.
(36) van Wüllen, C. *J. Chem. Phys.* **1998**, *109*, 392−399.
(37) (a) Pantazis, D. A.; Chen, X. Y.; Landis, C. R.; Neese, F. *J. Chem. Theory Comput.* **2008**, *4*, 908−919. (b) Pantazis, D. A.; Neese, F. *J. Chem. Theory Comput.* **2009**, *5*, 229−238.
(38) Gauss, J. In *Modern Methods and Algorithms in Quantum Chemistry*; Grotendorst, J., Ed.; John von Neumann Institute for Computing: Jülich, Germany, 2000; NIC series, Vol. *1*, pp 509−560.
(39) Hess, B. A.; Marian, C. M.; Wahlgren, U.; Gropen, O. *Chem. Phys. Lett.* **1996**, *251*, 365−371.
(40) Neese, F. *J. Chem. Phys.* **2005**, *123*, 034107/1.
(41) Weigen, F.; Häser, M. *Theor. Chem. Acc.* **1997**, *97*, 331−340.
(42) (a) Angeli, C.; Cimiraglia, R.; Evangelisti, S.; Leininger, T.; Malrieu, J. P. *J. Chem. Phys.* **2001**, *114*, 10252−10264. (b) Angeli, C.; Cimiraglia, R.; Malrieu, J. P. *J. Chem. Phys.* **2002**, *117*, 9138−9153.
(43) Neese, F. *J. Chem. Phys.* **2003**, *119*, 9428.
(44) Neese, F. *ORCA. An Ab Initio, Density Functional and Semiempirical Program Package*, Version 2.7; Universität Bonn: Bonn, Germany, 2010.
(45) (a) Wang, F.; Ziegler, T. *J. Chem. Phys.* **2004**, *121*, 12191. (b) Vahtras, O.; Rinkevicius, Z. *J. Chem. Phys.* **2007**, *126*, 114101.
(46) Neese, F.; Solomon, E. I. In *Magnetoscience—From Molecules to Materials*; Miller, J. S., Drillon, M., Eds.; Wiley-VCH Verlag GmbH: Weinheim, Germany, 2003; Vol. *IV*, pp 345−466.
(47) Jørgensen, C. K. *Absorption Spectra and Chemical Bonding in Complexes*; Pergamon Press in Oxford: New York, 1962; p 159.
(48) Bendix, J.; Brorson, M.; Schäffer, C. E. *Inorg. Chem.* **1993**, *32*, 2838−2849.
(49) Krzystek, J.; Ozarowski, A.; Telser, J. *Coord. Chem. Rev.* **2006**, *250*, 2308−2324.
(50) Collingwood, J. C.; Day, P.; Denning, R. G. *J. Chem. Soc., Faraday Trans. 2* **1973**, 591−607.
(51) Atanasov, M.; Rauzy, C.; Baettig, P.; Daul, C. *Int. J. Quantum Chem.* **2005**, *102*, 119−131.
(52) Mossin, S.; Weihe, H.; Barra, A.-L. *J. Am. Chem. Soc.* **2002**, *124*, 8764−8765.